Effects of planning variables on urban traffic noise at different scales

Jiaxun Song[a], Qi Meng[a*], Jian Kang[b], Da Yang[a], Mengmeng Li[a]
a Key Laboratory of Cold Region Urban and Rural Human Settlement Environment Science and Technology, Ministry of Industry and Information Technology, School of Architecture, Harbin Institute of Technology, Harbin 150001, 66 West Dazhi Street, Nan Gang District, Harbin, China
b UCL Institute for Environmental Design and Engineering, The Bartlett, University College London (UCL), London WC1H 0NN, UK
* Corresponding author
Professor Jian Kang, UCL Institute for Environmental Design and Engineering, The Bartlett, University College London (UCL), London WC1H 0NN, UK
Email: j.kang@ucl.ac.uk

Abstract
This study examines the control of traffic noise in urban planning, considering the differences in noise impacts at various scales. Acoustic simulations and spatial statistics were employed to compare traditional planning variables and planning big data for noise analysis. The study investigates noise impact in urban centres and fringes and analyses varying effects of a given variable on traffic noise at scales of 300, 600, and 1200 m. Additionally, sound environment optimisation strategies are proposed and validated for different scales and areas. The major findings are: (1) planning big data had more impact in single-variable models, while traditional variables were more significant in multivariable models; (2) the noise impact of most variables varied with the area and scale, for example, at 1200 m, the total building perimeter has opposing effects in urban centres and fringes, and the greening rate changes from positive to negative with increasing scale; (3) the proposed strategies reduced traffic noise by an average of 4.2, 3.2, and 2.3 dB at scales of 300, 600, and 1200 m, respectively. These findings provide valuable insights for the optimisation of urban sound environments.

Keywords: Multi-scale, planning factors, traffic noise, urban acoustic environment.

2024 Sustainable Cities and Society
Date received: 8 June 2023 Date accepted: 14 October 2023
Available online: 16 October 2023

1. Introduction

Urban planning and design play a crucial role in multiple environmental fields and are integrally connected to factors such as residents' activities, the urban microclimate, and morphological urban patterns (Ding et al., 2023; Lei et al., 2021; Luo and He, 2021; Yiannakou and Salata, 2017; Yin et al., 2018). The issue of traffic noise ranking as the second-largest global environmental concern (Zhang et al., 2023), affecting people's health and working efficiency (Meng et al., 2021; Swinburn et al., 2015). Consequently, it is intricately linked with urban planning and design (Rey Gozalo et al., 2016). As a result, controlling noise in urban areas through spatial planning is widely acknowledged as an effective strategy (Barrigon Morillas et al., 2018). China's *'Urban Planning Compilation Measures'* published in 2005, identified urban planning as a crucial public policy instrument for managing spatial resources, specifying that traffic noise, as a detrimental spatial factor, should be considered in planning frameworks. Additionally, the *'Technical Policy for the Prevention and Control of Ground Traffic Noise Pollution'* issued in 2010, accentuates the importance of sound regional development planning and transport planning as essential methods for the management and mitigation of traffic noise pollution.

Numerous studies have advanced methods for mitigating traffic noise through urban planning (Hong and Jeon, 2017; Tang and Wang, 2007; Yu and Kang, 2017), achieving macro-level control over this environmental issue. Concurrently, the concept of smart cities has gained strategic importance in recent years (Borsekova et al., 2018). In the United States, an interdisciplinary consortium comprising civic leaders, data scientists, and technologists has focused on building "Smart Cities"—urban environments equipped with an infrastructure dedicated to the optimised collection and utilisation of data to enhance the quality of life for residents (2015). In China's Thirteenth Five-Year Plan, unveiled in 2016, the nation advocated for the establishment of a series of new smart cities as demonstration projects.

The developing field of smart cities has rendered urban planning increasingly nuanced, propelling it into a new phase of problem-solving strategies for urban environments. For instance, extant research has leveraged data sets from automatic smart card fare collection systems to elucidate a city's spatial structure and track its temporal changes (Zhong et al., 2014). Additional studies have employed social media data to capture Beijing's urban image (Peng et al., 2020), utilised mobile phone data to investigate urban vibrancy in Shenzhen (Tang et al., 2018), and analysed massive GPS trajectory data to understand the traffic patterns of cities (Wang et al., 2020). These examples illustrate that big data offers quantitative backing for urban planning initiatives. By gathering and analysing the wealth of information embedded in big data, it is possible to extract overarching principles of urban planning, thereby effectively steering both planning and design strategies. In this context, the collection of big data pertinent to urban planning for the purpose of controlling traffic noise emerges as a promising and efficient approach.

The integration of big data is poised to enhance the precision of traffic noise control. Therefore, noise maps generated at various scales—ranging from specific streets and urban areas to entire cities—will possess increased applicability. In collaborative efforts, governmental bodies have partnered with researchers to undertake multi-scale acoustic mapping studies, thereby facilitating improved noise management across nations and regions while identifying viable applications within smart cities. For example, Luca Maria Aiello et al. (2016) employed Flicker data to construct soundscape maps for major cities like London and New York, annotating the dominant sounds along each road to enable customised auditory experiences for travellers. Aletta et al. (2015) offered acoustical guidance for future urban design interventions by creating a soundscape map of Brighton's Valley Garden; they marked acoustic features at specific measurement points through sound walks and then applied interpolation methods to generate a comprehensive soundscape map for the entire area. Additional research utilised Cadna/A noise simulation software to model urban street traffic noise, formulate noise maps, and recommend specific strategies such as traffic volume reduction and alteration of road surfaces from smooth asphalt to porous materials for noise control (Popescu et al., 2011).

These case studies underscore the directive utility of acoustic maps across different scales. At the urban scale, acoustic maps contribute to the controllability of expansive acoustic environments. Maps generated for specific urban areas offer intuitive insights into the acoustic characteristics of those zones, thereby informing subsequent planning and design endeavours. Meanwhile, street-scale noise maps furnish detailed guidelines for building and road design, focusing on elements like construction materials and facade characteristics. Consequently, an examination of the influence of planning variables on traffic noise across these various

scales is critically important for the creation of multi-scale traffic noise maps.

To deepen the understanding of the role of planning big data in noise control and furnish a theoretical foundation for noise management at multiple scales with increased precision, this study has been initiated. The fundamental objective of this study is to assess the impact and examine the differences between traditional planning variables and planning big data on traffic noise levels at varying scales in diverse urban areas. The research questions are posited as follows:

(1) Which type of data, traditional planning variables or planning big data, is more suitable for traffic noise analysis at various scales?

(2) What are the differences in the impacts of a given planning variable on traffic noise between urban centres and fringe areas?

(3) What are the differences between the impacts of a given planning variable on traffic noise at the building, semi-block, and block scales?

These questions guide the current study and aim to resolve critical issues in the realm of urban noise management through planning and design.

2. *Literature Review*

Previous studies have extensively examined various types of planning variables affecting noise, such as buildings and block morphology, road morphology, landscape morphology, and land-use indicators. For example, Montalvao Guedes et al. (2011), Margaritis and Kang (2014) determined that construction density, open spaces, green space density, and land-use classes were highly correlated with noise levels. Based on previous studies. Hong and Jeon (2017) included water feature indicators as a separate category and assessed the impact of water feature components on the soundscape. Certain studies have verified the correlation between planning indicators and traffic noise based on four aspects (Ryu et al., 2017; Salomons and Pont, 2012; Silva et al., 2018; Weber et al., 2014): buildings, roads, landscapes, and land-use categories, including indicators of construction height, total built area, road area density, the fraction of industrial area, and sky view factor. In this study, these are categorised as traditional planning variables. More recently, the utilisation of big data has garnered considerable research attention for planning smart cities. Certain studies explored the impact of space syntax variables and point of interest (POI) data on traffic noise. In principle, space syntax describes the relationship between space and human society and can be used to quantify urban road network structures (Bafna, 2003), whereas POI data reflect urban land functions or land-use classes (Tang et al., 2018). Dzhambov et al. (2014) proposed that space syntax theory can enhance noise prediction ability, and using LimA software, demonstrated that space syntax variables can effectively improve the accuracy of noise prediction. Mohareb and Maassarani (2019) further reported that although space syntax variables were correlated with the noise level, they varied across functional areas. However, most existing research examined the impact of traditional planning variables on noise, and only a few studies have explored the correlation between spatial syntax, POI big data, and noise. To date, no research has compared the applicability of traditional planning variables and planning big data to analyse traffic noise at different scales. Therefore, in our work, their effects on traffic noise are further compared using correlation analyses and spatial statistical methods to construct a more accurate noise prediction model in future research.

Prior research demonstrated that the impact of planning variables on noise varies across the types of urban areas. For example, Weber et al. (2014) distinguished that areas with high patch density and the most heavily built urban structure types (edge density) were associated with much higher noise exposure levels than less dense and less developed areas. Mohareb and Maassarani (2019) determined that the correlation between the spatial syntax variables and soundscapes varies across the land-use classes. Only a few studies have examined the variations in the impacts of planning variables on traffic noise at various urban areas. To address this research gap, the present study partitions the area under examination, as well as the validation area, into urban centres and urban fringes based on their urban master plans. The research thus aims to explore how planning variables differentially affect traffic noise levels in these distinct urban settings.

Although several studies have examined the effect of planning variables on traffic noise, only a few studies focused on the scale effect (Jackson and Fahrig, 2015). For instance, Margaritis and Kang (2016) explored the effectiveness of various urban planning variables at the micro-, meso-, and macroscale grid size (250, 500, and 1000 m, respectively) and determined that the features of urban morphology were uniquely related to the traffic noise levels at each scale. They proposed that the research scale is a key factor affecting

the correlation (Margaritis, 2016). Margaritis and Kang (2017) further studied the various impacts of greenspace indicators at the aggregation, urban, and kernel levels. However, only a few multiscale studies have been conducted in the field of noise, and the existing literature on multiscale noise research has not explored the variations of the impact of the same planning variable on noise at varying scales. This study aims to fill this void by evaluating the impact of a given planning variable on traffic noise at three scales—300 m, 600 m, and 1200 m. It further proposes planning and design strategies tailored for noise control at these scales and assesses the effectiveness of these interventions.

3. Methodology

3.1. Research framework

The research framework of this study is illustrated in Fig. 1. Based on the three research questions, the variables were extracted, and various scale grids were set, as detailed in Section 3. Thereafter, the research content and the methodology followed to answer these three research questions are discussed in Sections 4.1, 4.2, and 4.3. Finally, in Section 4.4, we proposed the sound environment optimisation strategies based on the analysis and verified the feasibility and generalisation of the strategies.

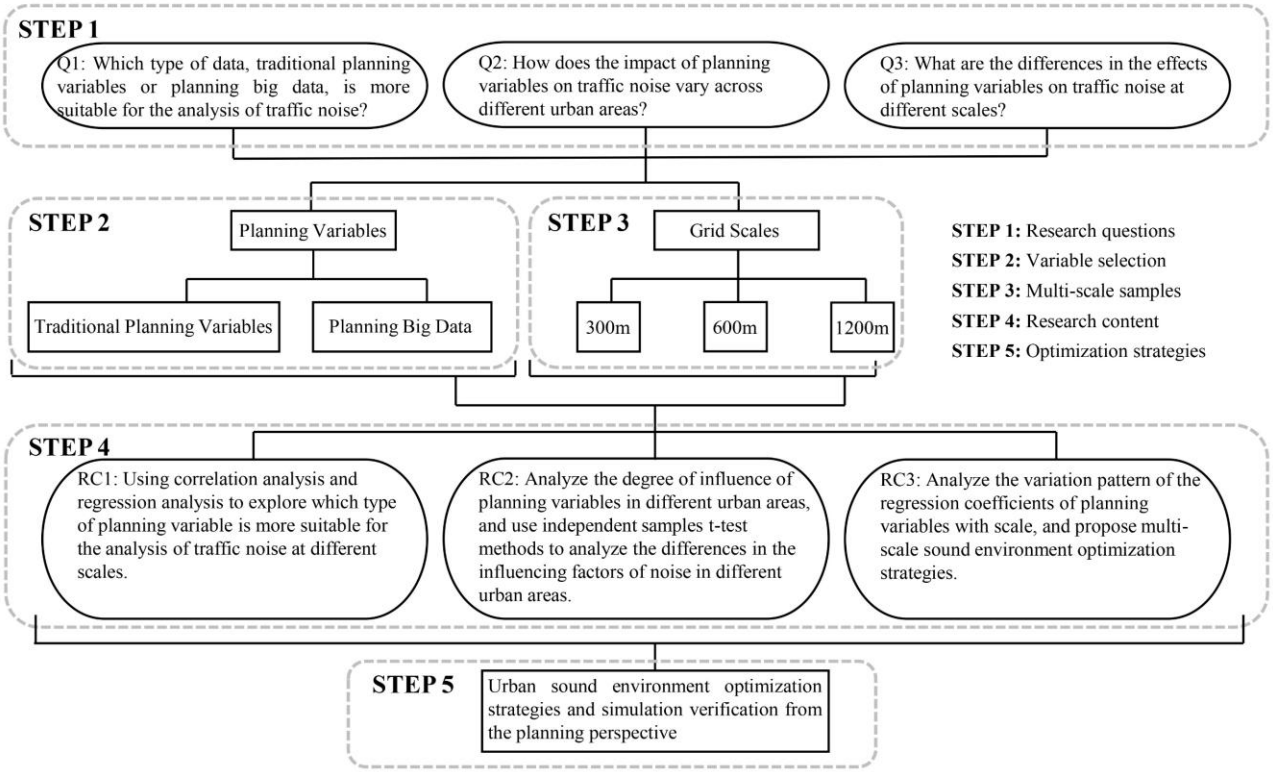

Fig. 1. Research framework

3.2. Study area and scale division

The *Annual Report on Prevention and Control of Noise Pollution in China 2022* identified Guangdong Province as a key area of focus for environmental supervision, with noise complaints accounting for approximately 22.5% of all ecological and environmental grievances. This designation highlights the importance of addressing noise control in Guangdong Province. Dongguan City, a newly designated first-tier city in the Guangdong Province, plays a pivotal role in integrating ports and urban rail transit in the region. Notably, the city faces significant traffic noise challenges due to high traffic volume in the suburbs and frequent activities in the urban centre. To investigate these issues, our study specifically selected regions within Dongguan City as research targets (Fig. 2a). The research area encompasses the northwest region of Dongguan City (Fig. 2b). It also includes central urban areas such as Guancheng, Dongcheng District, Nancheng District, and Wanjiang District, as well as urban fringe areas such as the western part of Liaobu Town and the southern part of Gaobu (Fig. 2c). These regions are classified as urban centres and urban fringes, respectively, according to the *Master Plan for the Territorial Space of Dongguan (2022–2035)*. Geographically, the urban centre lies between 113°702′E and 113°825′E longitude and 22°994′N and

23°070′N latitude (WGS1984 coordinate system). For the classification of roads within the research area, the study adheres to the guidelines set forth in the *Technical Standard of Highway Engineering (JTGB01-2019)*. This standard delineates roads into four service levels: first, second, third, and fourth, with designated speeds of 120 km/h, 80 km/h, 40 km/h, and 30 km/h respectively. Notably, the first-level roads are considered intercity freeways. However, since the scope of this study is confined to the urban territory of Dongguan, first-level roads are excluded. Consequently, roads within the research area are categorised into three service levels: second, third, and fourth, as shown in Fig. 2c.

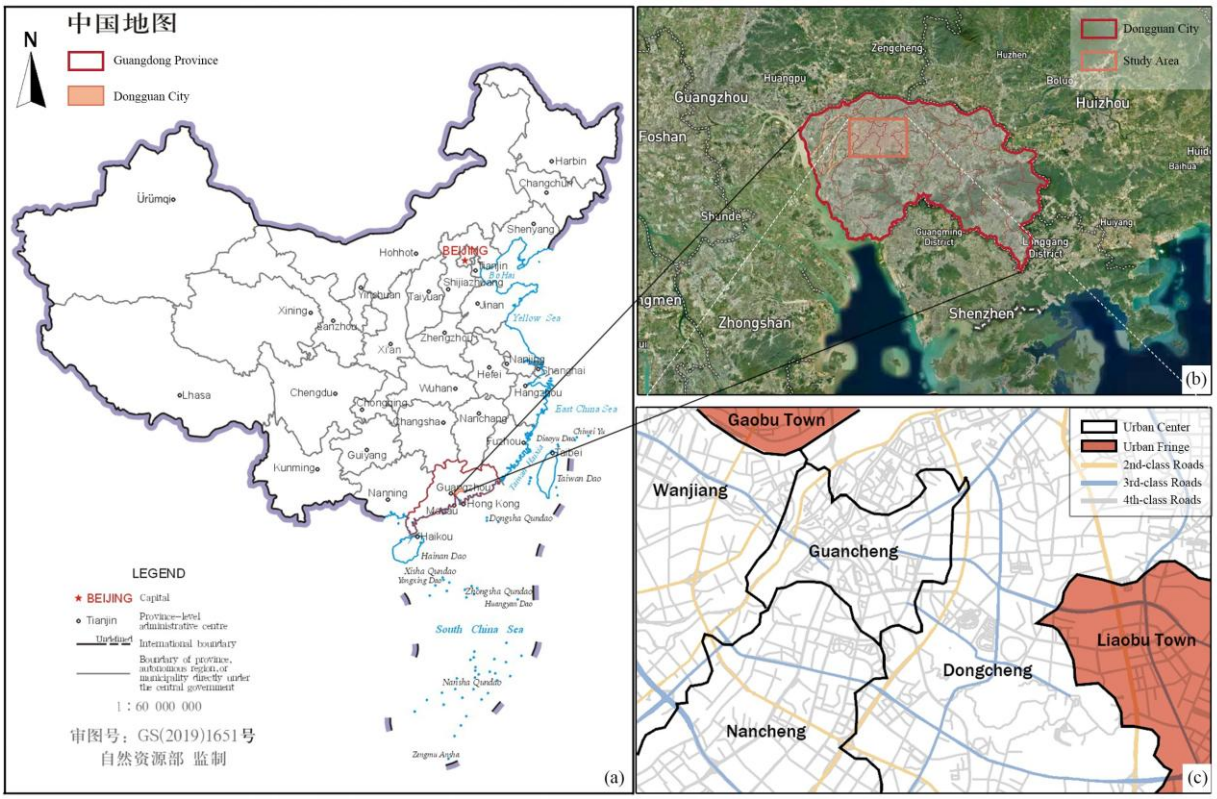

Fig. 2. Study area (source of Fig. 2a: Standard Map Service System http://bzdt.ch.mnr.gov.cn/index.html/)

The grids utilised in this study were adjusted to align with the planning characteristics of grids employed in previous research (Margaritis and Kang, 2016; Ryu et al., 2017). According to the *Standard for Urban Residential Area Planning and Design (GB50180-2018)*, a basic residential unit should have a scale ranging from 150 to 250 m. To capture the influence of planning variables comprehensively and at different scales in urban planning and design processes, we selected three grid scales: 300, 600, and 1200 m, representing the building, semi-block, and block scales, respectively (Fig. 3). These scales facilitated a more comprehensive and differentiated analysis of the planning variables, and supported decision-making across various scales. The fishnet command in ArcGIS was employed to establish complete coverage of the study area with grids of these three scales.

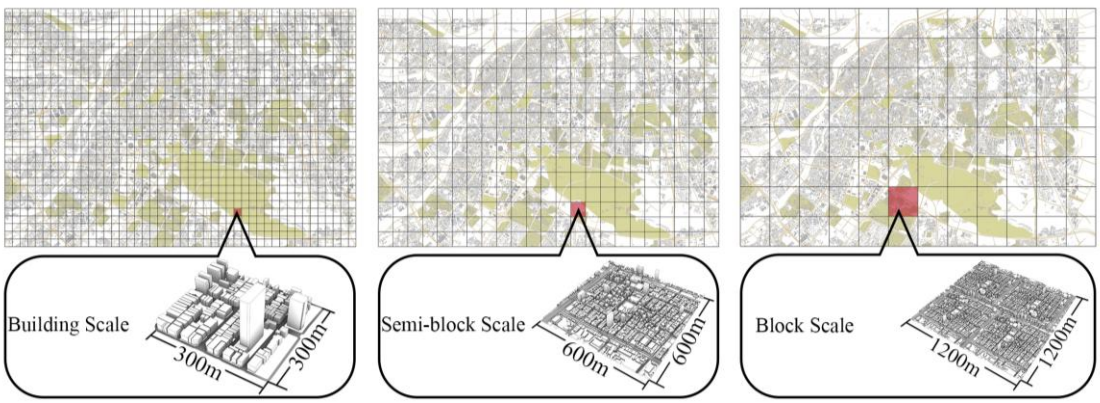

Fig. 3. Scale division

3.3. Selection of planning variables

This study incorporates planning indicators from previous studies and categorizes them into two types (Dzhambov et al., 2014; Hao et al., 2015; Hong and Jeon, 2017; Huang et al., 2021; Lam et al., 2013; Margaritis, 2016; Margaritis et al., 2016; Margaritis and Kang, 2014; Margaritis and Kang, 2016; Margaritis and Kang, 2017; Margaritis et al., 2020; Margaritis et al., 2018; Mohareb and Maassarani, 2019; Montalvao Guedes et al., 2011; Ryu et al., 2017; Salomons and Pont, 2012; Silva et al., 2018; Tang and Wang, 2007; Wang and Kang, 2011; Wang et al., 2018; Weber et al., 2014; Yu and Kang, 2017; Zhou et al., 2017): traditional planning variables and planning big data. Traditional planning variables encompass urban morphology variables that have been demonstrated to be associated with traffic noise in previous research (Dzhambov et al., 2014; Hong and Jeon, 2017; Margaritis, 2016; Margaritis et al., 2016; Margaritis and Kang, 2014; Mohareb and Maassarani, 2019; Montalvao Guedes et al., 2011; Ryu et al., 2017; Salomons and Pont, 2012; Wang and Kang, 2011; Weber et al., 2014), including building morphology, road morphology, and landscape indicators. Planning big data, conversely, refers to data reflecting spatial planning characteristics within the framework of smart cities (Wang and Yin, 2023), including spatial syntax variables and POI big data. Spatial Design Network Analysis (sDNA) was employed to calculate space syntax variables (Cooper and Chiaradia, 2020; Ma, 2020). Based on the concept of the ‘15-min living circle’ (Wu et al., 2021), this study selected spatial syntax variables of 1200 m Closeness, 1200 m Betweenness, 8000 m Closeness, and 8000 m Betweenness, representing road accessibility within a 15-min walk, pass-through probability within a 15-min walk, road accessibility within a 15-min drive, and pass-through probability within a 15-min drive, respectively. Furthermore, specific POI categories closely related to population flow and traffic distribution (Alhazzani et al., 2021), namely transportation, financial services, science and education, parking lots, leisure facilities, medical services, and accommodation services, were used to represent land-use classes in the urban space (Tang et al., 2018). Table 1 provides an overview of the selected planning variables and their meanings.

Table 1. Selected planning variables.

Types	Subtypes	Parameter	Formula	Definition
Traditional Planning Variables	Building	BD	BD = $\frac{\sum A_{BA}}{A_C}$. A_{BA} is the base area of a building in one cell. A_C is the area of a single cell.	Building density
		VR	VR = $\frac{GFA}{A_C} = \frac{\sum(A_{BA} \times N_S)}{A_C}$. A_{BA} is the base area of a building in one cell. N_S is the number of storeys of the building. GFA is the total building areas in a cell. A_C is the area of a single cell.	Volume ratio
		BP_SUM	BP_SUM = $\sum P_{BA}$. P_{BA} is the base perimeter of a building in the cell.	Total building perimeters
		BP_AVG	BP_AVG = $\frac{BP\_SUM}{n} = \frac{\sum P_{BA}}{n}$. P_{BA} is the base perimeter of a building in the cell. n is the number of the buildings. BP_SUM is the total building perimeter in the cell.	Average perimeter of buildings
		BA	BA = $\sum A_{BA}$. A_{BA} is the base area of a building in one cell.	Building area
		BS	BS = $\frac{\sum N_S}{n}$. N_S is the number of storeys of a building. n is the number of the buildings.	Building storey
		GFA	GFA = $\sum(A_{BA} \times N_S)$. A_{BA} is the base area of a building in one cell. N_S is the number of storeys of the building.	Gross floor area
	Road	RL	RL = $\frac{\sum L}{n_r}$. L is the length of a road in the cell. n_r is the number of the roads.	Road length
		NUM_IN	NUM_IN = $\sum N_{IN}$. N_{IN} is the number of the intersections in one cell.	The number of intersections
	Landscape	GR	GR = $\frac{\sum A_G}{A_C}$. A_G is the area of a green space in urban in one cell. A_C is the area of a single cell.	Greening rate (urban)
Planning Big Data	Space Syntax Variables	NQPDA1200	$NQPDA\ (x) = \sum_{y \in Rx} \frac{P\ (y)}{d\ (x,y)}$. P (y) is the proportion of link y within the radius of R, d (x,y) is the shortest topological distance from link x to link y; Rx is the set of links in the network	Closeness (R = 1200 m)- the road accessibility of walking for 15 min.

		Euclidean radius R from link x; NQPDA (x) is the integration of the road network within searching radius of R (Ma, 2020); R = 1200 m	
	TPBtA1200	$OD\ (y,z,x) = \begin{cases} 1, if\ x\ is\ on\ the\ goedesic\ from\ y\ to\ z \\ 1/2, if\ x \equiv y \not\equiv z \\ 1/2, if\ x \equiv z \not\equiv y \\ 1/3, if\ x \equiv y \equiv z \\ 0, otherwise \end{cases}$ $TPBtA\ (x) = \sum_{y \in N} \sum_{z \in Ry} OD\ (y,z,x) \frac{P\ (z)}{Links\ (y)}$ OD (y,z,x) is the shortest topological distance through link x between link y and z within searching radius of R; P (z) is the proportion of link z within the radius of R; Links (y) is the number of links in radius of R from each link y; Ry is the set of links in the network Euclidean radius R from link y; N is the set of links in the global spatial system; TPBtA (x) is the betweenness of the road network within the searching radius of R (Ma, 2020); R = 1200 m	Betweenness (R = 1200 m)- the probability of a road being passed through within the area range of walking for 15 min.
	NQPDA8000	R = 8000 m. Others same as 'NQPDA1200'	Closeness (R = 8000 m)- the road accessibility of driving for 15 min.
	TPBtA8000	R = 8000 m. Others same as 'TPBtA1200'	Betweenness (R = 8000 m)- the probability of a road being passed through within the area range of driving for 15 min.
POIs	NUM_T	NUM_T = $\sum N_T$. N_T is the number of transportation POIs in the cell.	The number of traffic POIs
	NUM_F	NUM_F = $\sum N_F$. N_F is the number of financial service POIs in the cell.	The number of finance POIs
	NUM_SE	NUM_SE = $\sum N_{SE}$. N_{SE} is the number of scientific and educational POIs in the cell.	The number of education POIs
	NUM_P	NUM_P = $\sum N_P$. N_P is the number of parking lot POIs in the cell.	The number of parking POIs
	NUM_L	NUM_L = $\sum N_L$. N_L is the number of leisure and entertainment POIs in the cell.	The number of leisure POIs
	NUM_M	NUM_M = $\sum N_M$. N_M is the number of medical service POIs in the cell.	The number of medical POIs
	NUM_A	NUM_A = $\sum N_A$. N_A is the number of accommodation service POIs in the cell.	The number of accommodation POIs

3.4. Extraction of variables

The process of extracting the independent and dependent variables is illustrated in Fig. 4.

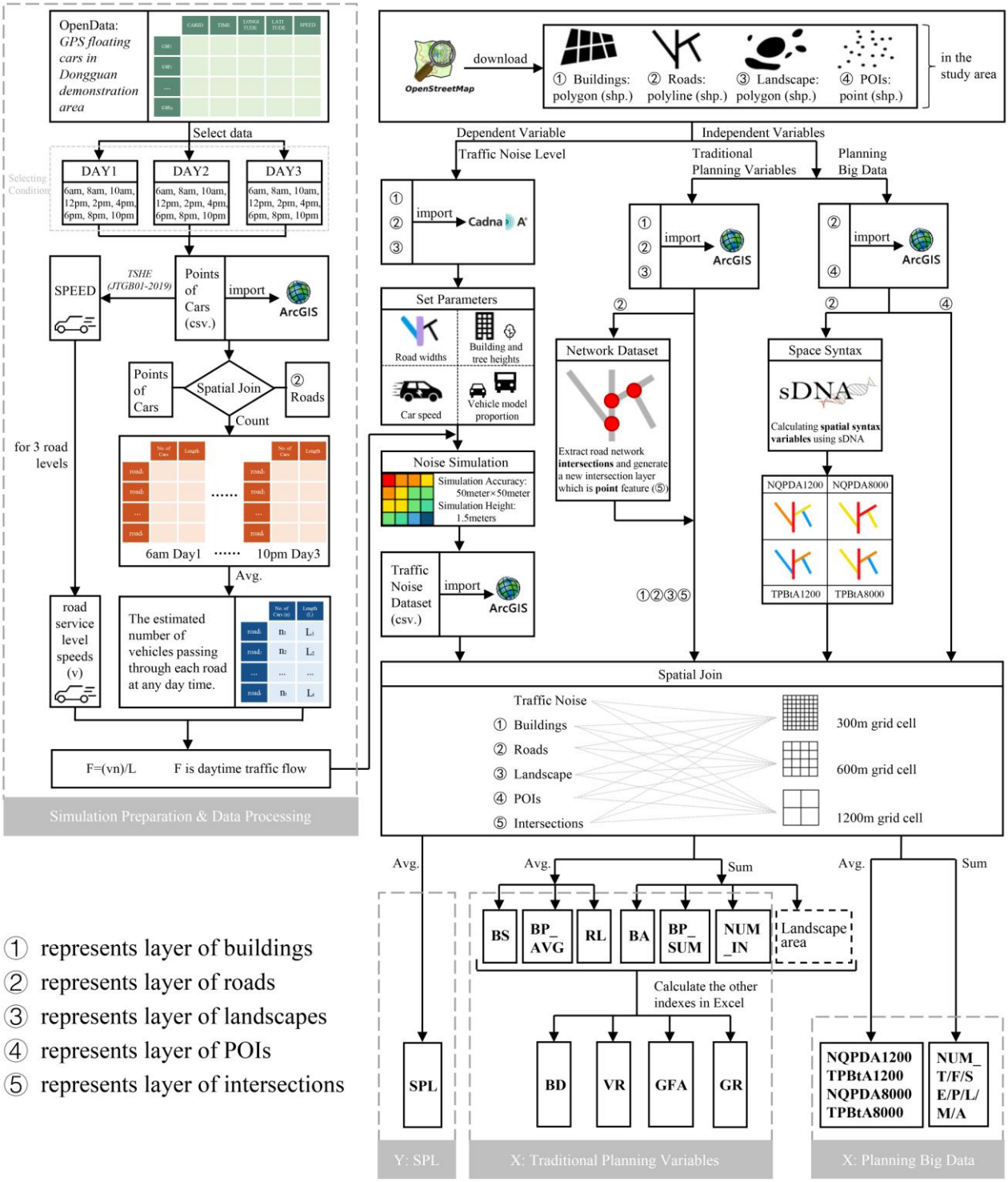

Fig. 4. Extraction process of independent and dependent variables

In this study, the noise database was established using the noise simulation software Computer-Aided Noise Abatement (Cadna/A), as Cadna/A simulations exhibit high accuracy (Suarez and Barros, 2014). The floating-car GPS open data from the Dongguan demonstration area were utilised to calculate traffic flow and simulate noise. The dataset comprises 24-h information for 3 d, including vehicle ID, signal time, longitude, latitude, speed, and direction. According to the *Law of the People's Republic of China on Prevention and Control of Environmental Noise Pollution (2021)*, the 'daytime' is defined as the period between 6:00 and 22:00. Based on a previous study (Levinson, 2022), which emphasised the need to establish

relationships between traffic flow, traffic density, and traffic velocity, the equation for calculating equivalent hourly flow was employed.

$$F = kv = vn/L \ (/h).$$

F denotes the equivalent hourly flow; *v* represents the vehicle speed (km/h); k denotes the density of vehicles per kilometre; *n* represents the number of vehicles on the road; and *L* indicates the road length.

To estimate average daytime traffic on the roads, the number of vehicles passing through each road was collated at nine discrete daytime intervals (6 a.m. to 10 p.m. every two hours) across a span of three days (*n*). Because vehicle speeds are subject to fluctuation, this study relied on road service level speeds (*v*) as specified in the *Technical Standard of Highway Engineering (JTGB01-2019)* for computational purposes. Specifically, second-level roads have a designated speed of 80 km/h, third-level roads 40 km/h, and fourth-level roads 30 km/h (Fig. 2c). Existing literature supports the use of these road service level speeds as adequate predictors of noise impact (Su et al., 2022). However, the correlation between road speed and traffic volume also necessitates empirical verification (Su et al., 2022). To this end, this study calculated the average vehicle speed within the database, found to be 16.1 km/h, and employed this value to corroborate the accuracy of the vehicle count (*n*) passing through each road within a designated time frame. The road lengths (*L*) were calculated using the ArcGIS software. Consequently, the average daytime traffic flow for each road was calculated and input as a parameter into Cadna/A.

In terms of setting parameters in Cadna/A, the road width, car speed, and vehicle model proportion must be defined (Popescu et al., 2011). In order to acquire statistics for the proportion of vehicle models, random samples of 10 road sections for each road level within the study area were subjected to a three-day vehicular survey. This survey was conducted at the nine specified daytime intervals previously mentioned. The road width and car speed were determined based on the *Technical Standard of Highway Engineering (JTGB01-2019)*. Second-level roads had a width of 7.5 m and a car speed of 80 km/h, third-level roads had a width of 7 m and a car speed of 40 km/h, and fourth-level roads had a width of 6.5 m and a car speed of 30 km/h (Fig. 2c). In the model, the building height was consistently calculated as 2.8 m per story, following the *Residential Design Specification (GB50096-2011)*. Additionally, the heights of 30 trees along a typical urban road and in a city park in the study area were measured, with average heights of 3 and 10 m for street and park trees, respectively. These heights were assigned to the landscape layer of Cadna/A. Subsequently, the defined parameters were inputted to Cadna/A to simulate the plane traffic noise in the study area, with a simulation accuracy of 50 m and a noise simulation height of 1.5 m (Meng et al., 2020). The noise dataset was spatially joined with grids of 300, 600, and 1200 m to calculate the average noise value and obtain the sound pressure level of daytime traffic noise (SPL) (Kothari et al., 2016).

To extract the independent planning variables, the data of building, road, landscape, and POI were obtained from OpenStreetMap (OSM) and imported into ArcGIS. The elements were transformed into geometric shapes, with road network intersections extracted using the Network Analyst toolbox and Network Dataset method (Margaritis and Kang, 2016). The traditional planning variables were calculated by spatially joining the building, road, landscapes, and intersection layers with fishnets, utilising ArcGIS to calculate the polygon areas, polyline lengths, and point numbers in each grid. This process yielded the values for building area (BA), building density (BS), total building floor area (BP_SUM), average building floor area (BP_AVG), road length (RL), number of road intersections (NUM_IN), and total landscape area per cell. Additional traditional planning variables such as building density (BD), visibility ratio (VR), gross floor area (GFA), and green ratio (GR) were calculated using the formulae listed in Table 1. To plan the big

data, the Closeness and Betweenness values were calculated for the road layer. Subsequently, the road and POI layers were spatially joined with fishnets to calculate the average space syntax variable values and the number of POIs in each category within each cell (Kothari et al., 2016).

Thus, the dependent variables of the daytime traffic noise level, as well as the independent planning variables, were extracted.

3.5. Statistical analysis

Numerous studies have confirmed that traffic noise is spatially heterogeneous and influenced by geographical location (Torija et al., 2011). To explore the influence of planning variables on traffic noise levels, this study employed spatial statistical methods, such as factor detection and geographically weighted regression (GWR) (Wang et al., 2016), as well as conducted Pearson correlation analysis and independent sample *t*-test. Pearson's correlation analysis was used to test the numerical correlation between the planning variables and traffic noise. The factor detector tested the influence weight of the planning variables on traffic noise spatial heterogeneity using the GD package in R language for analysis (Song et al., 2020). GWR studied the influence of multiple independent variables on traffic noise levels using a regression model, and all variables were standardised using SPSS in advance. The GTWR plug-in was used for the GWR experiment with the bandwidth parameter AICc and the kernel FIXED (Huang et al., 2010). The GWR results were calculated for three scales of 300 m, 600 m, and 1200 m. An independent sample *t*-test was used to verify whether the influence of planning variables on traffic noise levels exhibited significant differences across the urban regions.

4. Results and Discussion

4.1. Applicability analysis of traditional planning variables and planning big data at different scales

4.1.1. Correlation analysis of planning variables and traffic noise

This study analysed the applicability of planning variables from three perspectives. First, Pearson correlation analysis was conducted to examine the correlation between the planning variables and traffic noise, and the results depicted the similarity of their numerical trends. The results of the Pearson correlation analysis between the planning variables and the SPL are illustrated in Fig. 5.

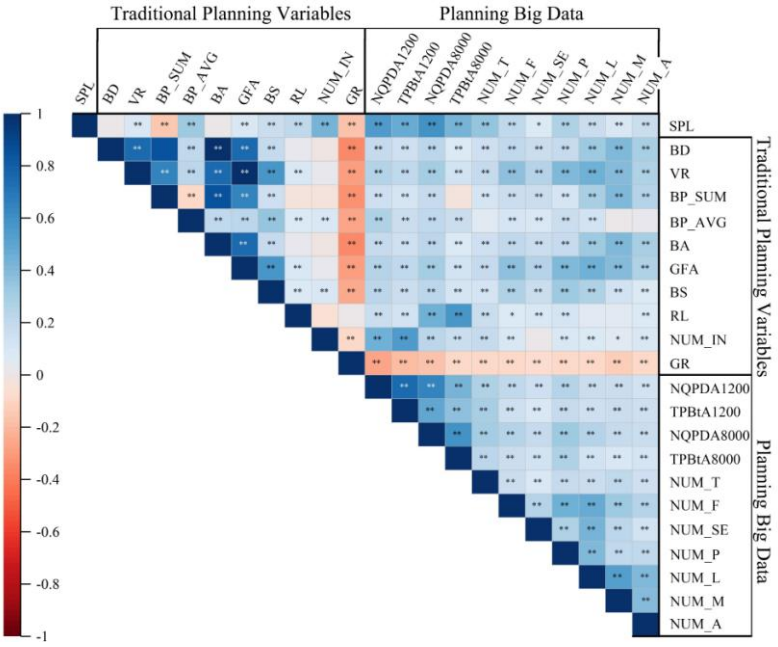

(a) 300 m

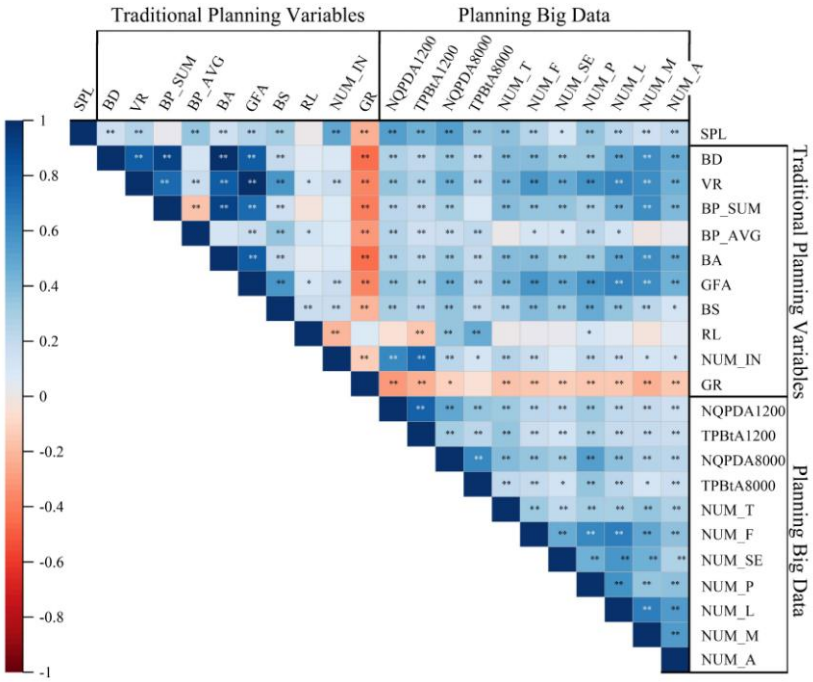

(b) 600 m

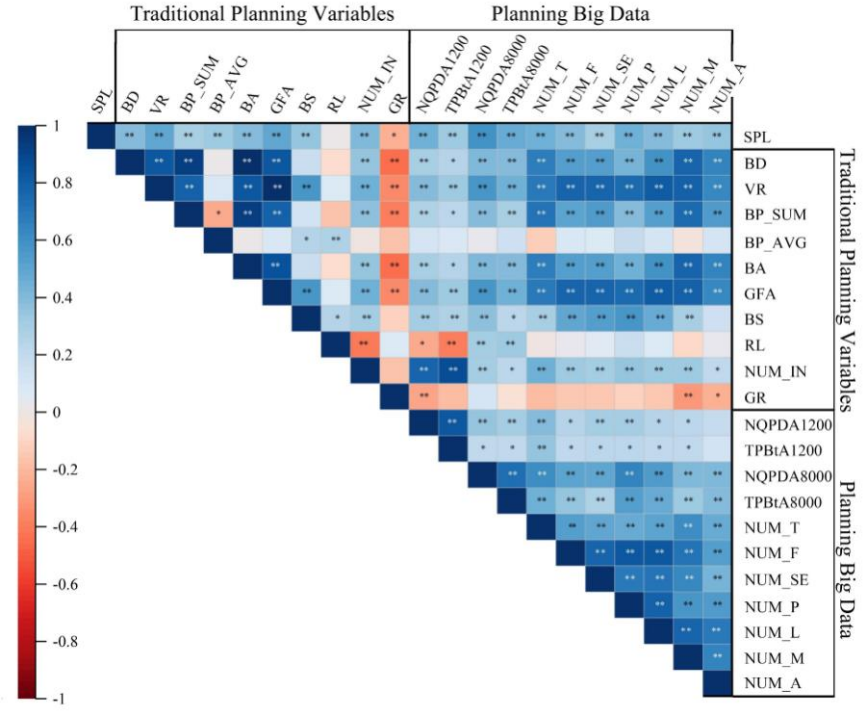

(c) 1200 m

** represents $p < 0.01$

* represents $p < 0.05$

Fig. 5. Results of Pearson correlation analysis

As depicted in Fig. 5, all planning big data exhibited a significant correlation with the SPL at each scale. Regarding the traditional planning variables, at the 300 m scale, BD and BA did not exhibit any correlation with SPL. At the 600 m scale, BP_SUM and RL demonstrated no correlation with SPL. At the 1200 m scale, RL was not correlated with SPL. Therefore, the correlation between planning big data and the SPL displayed greater significance than the traditional planning variables.

At the 300 m scale depicted in Fig. 5a, the correlation coefficient between NQPDA8000 and SPL was 0.58. This suggests that greater vehicular accessibility is associated with increased levels

of traffic noise. The correlation coefficient for GR was –0.18, indicating that an increase in urban greening can lead to a reduction in urban traffic noise, which aligns with the findings of previous studies (Margaritis et al., 2016). At this scale, the absolute value range of correlation coefficients between traditional planning variables and SPL was 0.0026–0.44, while for planning big data and SPL, it was 0.061–0.58. This indicates that at the 300 m scale, the correlation between planning big data and SPL was higher than that of traditional planning variables. For the 600 m scale, as illustrated in Fig. 5b, GR continued to exhibit a negative correlation with SPL, with a correlation coefficient of –0.22. The highest correlation was still observed between NQPDA8000 and SPL, reaching a coefficient of 0.54. At this scale, the absolute value range of correlation coefficients between traditional planning variables and SPL was 0.0017–0.49, while for planning big data and SPL, it was 0.11–0.54. Thus, at the 600 m scale, the correlation between planning big data and SPL remained higher than that between the traditional planning variables. Examining the 1200 m scale in Fig. 5c, SPL exhibited a significant negative correlation with GR, with a correlation coefficient of –0.23. However, SPL displayed a significant positive correlation with other planning variables. At this scale, the absolute value of correlation coefficients between traditional planning variables and SPL ranged from 0.0040–0.48, whereas for planning big data and SPL, it spanned within 0.30–0.58. These results indicate that at the 1200 m scale, the correlation between planning big data and SPL remains higher than that of traditional planning variables. Interestingly, the correlation between BP_SUM and SPL demonstrated a significant negative correlation at the 300 m scale, no significant correlation at the 600 m scale, and a significant positive correlation at the 1200 m scale. Previous studies confirmed that as the complete aspect ratio (CAR)[*] of buildings in an area increases, the sound level at L_{60} decreased before increasing slightly (Hao et al., 2015). This phenomenon observed in the present study can be explained as follows: at the 300 m scale, BP_SUM is within a small range of values, and as the CAR increases, it exhibits a negative correlation with the SPL. As the scale increased, BP_SUM in the grid cell increased, and CAR became positively correlated with SPL. At the 600 m scale, BP_SUM displayed no correlation with SPL, lying within the transitional range from negative to positive correlation.

4.1.2. Analysis of the influence weight of planning variables on the spatial heterogeneity of traffic noise

The influence weight of traditional planning variables and planning big data variables on the spatial heterogeneity of traffic noise was examined using the spatial statistical method of the Factor Detector. This analysis determined the moderate similarity between the spatial distributions of planning variables and traffic noise. The results of the Factor Detector are presented in Fig. 6.

Upon comparing Figs. 6a and 6b, it is evident that planning big data displays a considerably greater influence on the spatial heterogeneity of the SPL than traditional planning variables. In Fig. 6a, among the traditional planning variables, VR demonstrated a significant influence on the spatial heterogeneity of SPL at the 600 m scale, BP_SUM at the 300 m scale, BP_AVG only at 300 m, BA at both 300 and 600 m scales, and RL at 300 m. However, as depicted in Fig. 6b, the planning big data variables demonstrated considerable influence on the spatial heterogeneity of SPL. Specifically, NQPDA1200 was significant at 300 m, TPBtA1200 at both 300 and 600 m scales, NQPDA8000 at 300 and 600 m, TPBtA8000 at 300 m and 600 m, NUM_T on traffic noise heterogeneity at 300 and 600 m, NUM_F at 300 and 600 m, NUM_SE at the 600 m scale, NUM_P at both 300 and 600 m scales, NUM_L at both 300 m and 600 m, NUM_M at 300 and 600 m, and NUM_A at 300 and 600 m in relation to traffic noise heterogeneity.

[*] $CAR = A_C/A_T = (A_W + A_r + A_G)/A_T$, A_C is the combined surface area of the buildings and exposed ground, A_W is the wall surface area, A_r is the roof area, A_G is the area of exposed ground, and A_T is the total plan area of the region of interest.

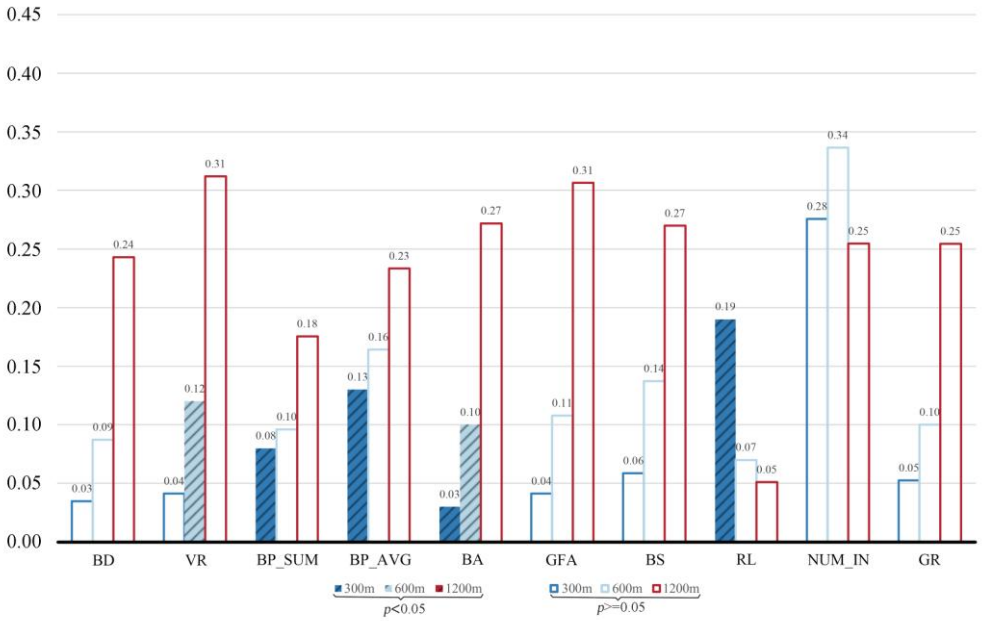

(a) Influence weight of traditional planning variables on spatial heterogeneity of SPL

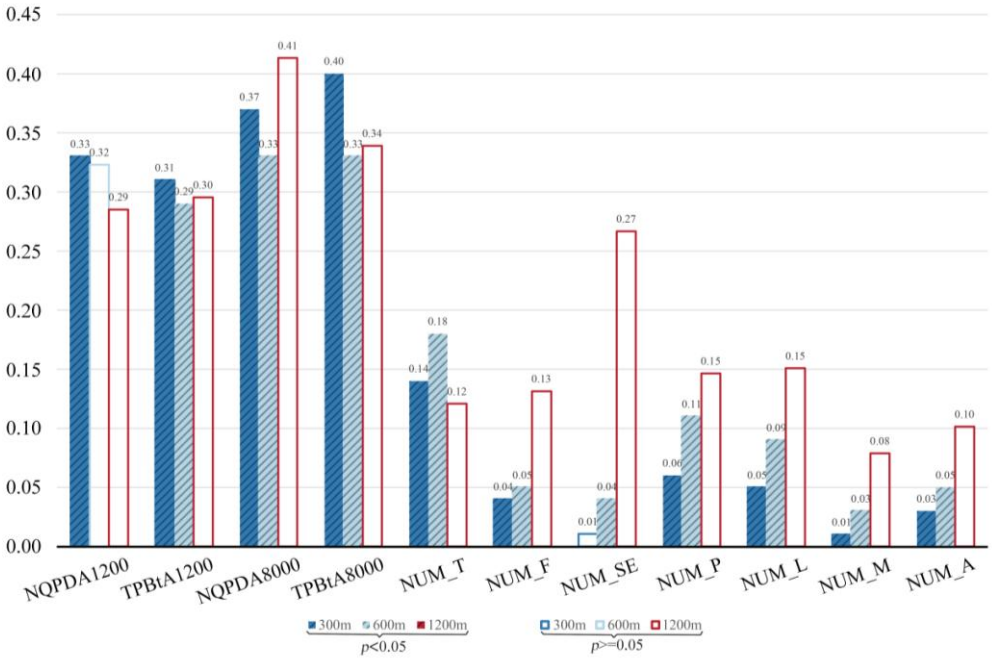

(b) Influence weight of planning big data on spatial heterogeneity of SPL

Fig. 6. Results of Factor Detector

4.1.3. Analysis of the influence degree of planning variables on traffic noise

Finally, GWR was employed to analyse the degree of influence of multiple planning variables on traffic noise. Table 2 presents the GWR models established at three scales: 300 m, 600 m, and 1200 m, providing an overview of the overall fit of the models.

Table 2. Overall fitting situation of GWR model.

	300 m	**600 m**	**1200 m**
R^2	76.02%	73.16%	74.58%
Adjusted R^2	75.70%	71.77%	69.05%
AICc	2498.32	758.71	231.07
Residual Squares	341.96	98.78	24.40
Independent variables in	BD, BP_SUM, BP_AVG, BS, GFA, RL, NUM_IN, GR,	BP_SUM, BP_AVG, BS, GFA, RL, NUM_IN, GR,	BD, BP_SUM, BP_AVG, BS, RL, NUM_IN, GR,

the models	NQPDA1200, TPBtA1200, NQPDA8000, TPBtA8000, NUM_T, NUM_F, NUM_SE, NUM_P, NUM_L, NUM_M, NUM_A	NQPDA1200, TPBtA1200, NQPDA8000, TPBtA8000, NUM_T, NUM_F, NUM_SE, NUM_P, NUM_L, NUM_M, NUM_A	NQPDA1200, TPBtA1200, NQPDA8000, TPBtA8000, NUM_T, NUM_F, NUM_SE, NUM_P, NUM_L, NUM_M, NUM_A
Independent variables excluded due to collinearity	VR BA	VR BA BD	VR BA BD GFA

As illustrated in Table 2, several variables were excluded from the three regression models owing to collinearity. In the 300 m scale model, VR and BA were excluded, while in the 600 m scale model, VR, BA, and BD were excluded. Similarly, in the 1200 m scale model, VR, BA, BD, and GFA were excluded. The determination coefficients (R^2) of the regression models at the three scales were 76.02, 73.16, and 74.58%, respectively. Furthermore, the AICc decreased from 300 to 1200 m, indicating an improved model performance and a more concise parameter setting. Within the GWR models, each planning variable was assigned a regression coefficient in every grid cell at the 300, 600, and 1200 m scales. Figure 7 depicts the maximum, minimum, and average coefficients of each planning variable at each scale.

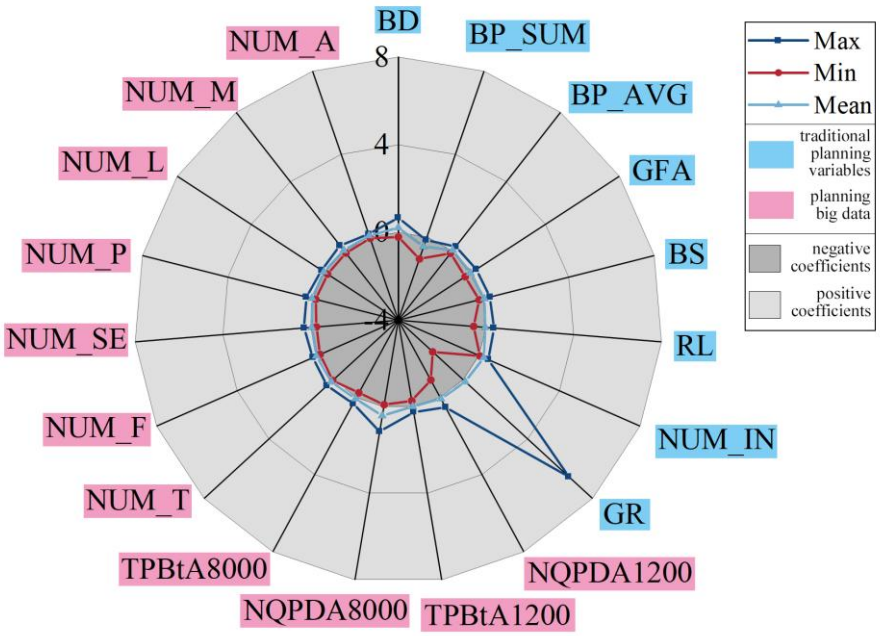

(a) 300 m

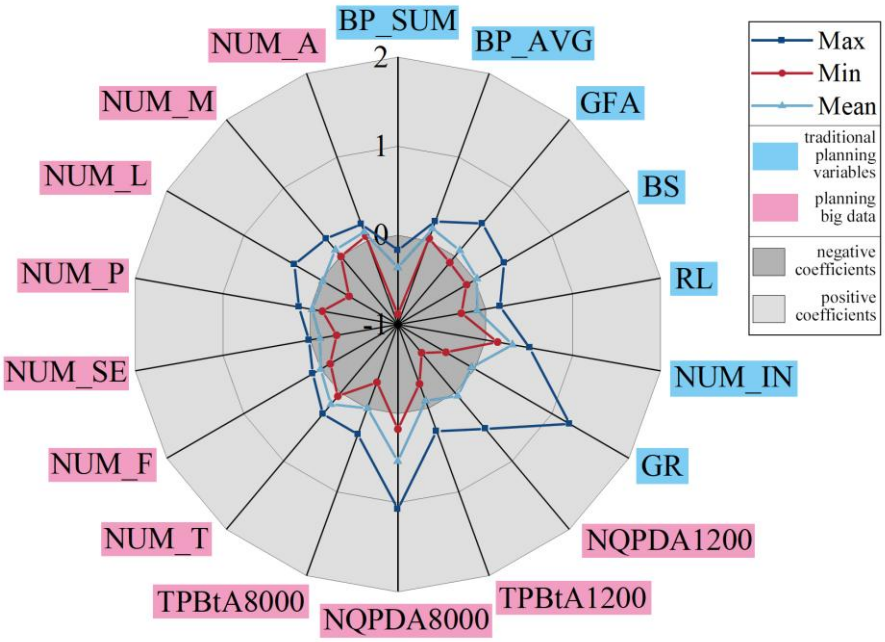

(b) 600 m

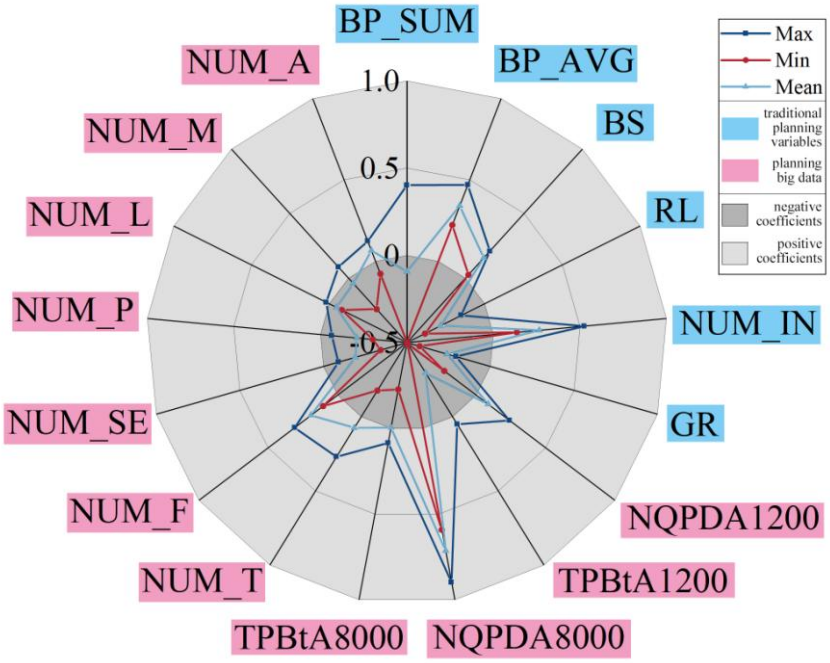

(c) 1200 m

Fig. 7. GWR coefficients of each planning variable at the scale of 300, 600, and 1200 m.

As depicted in Fig. 7a, at the 300 m scale, the average coefficients of each planning variable were similar, indicating a comparable influence on the SPL. Traditional planning variables exhibited an average impact ranging from 0.03 to 0.45, while planning big data variables ranged from 0.01 to 0.42. This suggests that planning big data had a slightly smaller average impact on SPL; however, NQPDA8000 posed a notable impact, represented by a regression coefficient of 0.42, second only to that of BP_SUM. In Figure 7a, the spike in the maximum GR coefficient indicates that, within the 300 m scale grid, GR has a substantial, positive influence on traffic noise in specific urban sectors. The urban area has a high building density and height, low coverage of second-level and third-level roads, and a high degree of greening rate. High building density, high building heights, and narrow roads can form "urban canyons" (Schiff et al., 2010), trapping and amplifying traffic noise. Progressing to Fig. 7b, at the 600 m scale, traditional planning variables forced an average impact on SPL ranging from 0.03 to 0.36. Among the planning big data

variables, NQPDA8000 had the greatest impact on big data, with a regression coefficient of 0.53. The remaining planning big data variables exhibited an average impact ranging from 0.0004 to 0.17, which was lower than that of the traditional planning variables, except for NQPDA8000. Finally, in Fig. 7c, at the 1200 m scale, traditional planning variables displayed an average impact on SPL ranging from 0.09 to 0.34. Similarly, NQPDA8000 provided the greatest impact on big data planning variables, with a regression coefficient of 0.71. The remaining planning big data variables posed an average impact ranging from 0.004 to 0.30, which was typically lower than that of the traditional planning variables, except for NQPDA8000.

Therefore, except for NQPDA8000, the average impact of planning big data on traffic noise in the regression model was generally lower than that of the traditional planning variables. The average impact of NQPDA8000 increased with scale, weakening the impact of other planning big data variables. Conversely, the impact of the traditional planning variables was less affected and remained more stable.

4.2. The difference in the impact of planning variables on traffic noise level in different urban areas

To explore the performance of planning variables in different urban areas and analyse the differences, this study employed an independent sample *t*-test to discuss the statistical differences in the impact of planning variables on traffic noise in urban centres and fringes. Four representative planning indicators were selected at each scale based on the results of Fig. 7 and the following selection criteria: (1) variables with the greatest impact, (2) variables with a large impact, and the GWR coefficients of the variables were positive and negative. Therefore, GR, RL, NQPDA8000, and BD were selected at 300 m; GR, GFA, NQPDA8000, and NUM_L at 600 m; NUM_IN, BP_SUM, NQPDA8000, and TPBtA1200 at 1200 m. All coefficient samples were imported into SPSS for the *t*-test to explore significant differences between the urban centre and fringe. The results are presented in Table 3.

Table 3. Results of independent sample *t*-test for each planning variable at the scale of 300, 600, 1200 m.

		***t*-value**	**df**	**Sig.**
300 m	BD**	4.157	1424.000	0.000
	GR**	8.511	585.927	0.000
	RL**	–16.330	179.645	0.000
	NQPDA8000**	9.849	1424.000	0.000
600 m	GFA	–1.903	366.000	0.058
	GR	–1.791	366.000	0.074
	NQPDA8000*	2.382	57.354	0.021
	NUM_L**	–7.208	41.868	0.000
1200 m	BP_SUM**	–3.936	17.493	0.001
	NUM_IN**	–3.849	94.000	0.000
	TPBtA1200**	2.714	94.000	0.008
	NQPDA8000**	–4.388	66.046	0.000

** represents $p < 0.01$

* represents $p < 0.05$

As indicated in Table 3, the BD, GR, RL, and NQPDA8000 displayed significant variations in the impact on SPL between the urban centre and fringe at the 300 m scale, with $p < 0.01$. At the 600 m scale, NQPDA8000 and NUM_L exhibited significant differences, whereas GFA and GR manifested no significant differences. At the 1200 m scale, NUM_IN, BP_SUM, NQPDA8000, and TPBtA1200 all exhibited significant differences. Therefore, the majority of the key planning variables displayed significant differences in their impact on traffic noise between the urban centre and the fringe.

In the GWR model, each planning variable yielded a regression coefficient for each grid cell. As depicted in Fig. 8, the coefficients are grouped by equal intervals and highlight the positive

and negative boundaries. The number of samples in each group was counted, and their proportions in the urban centre and fringe were calculated to analyse the differences. The vertical axis quantitatively represents the proportions of different coefficient ranges of one independent variable in the urban centre or fringe (PC/PF), and the horizontal axis represents the range of coefficient values (CR).

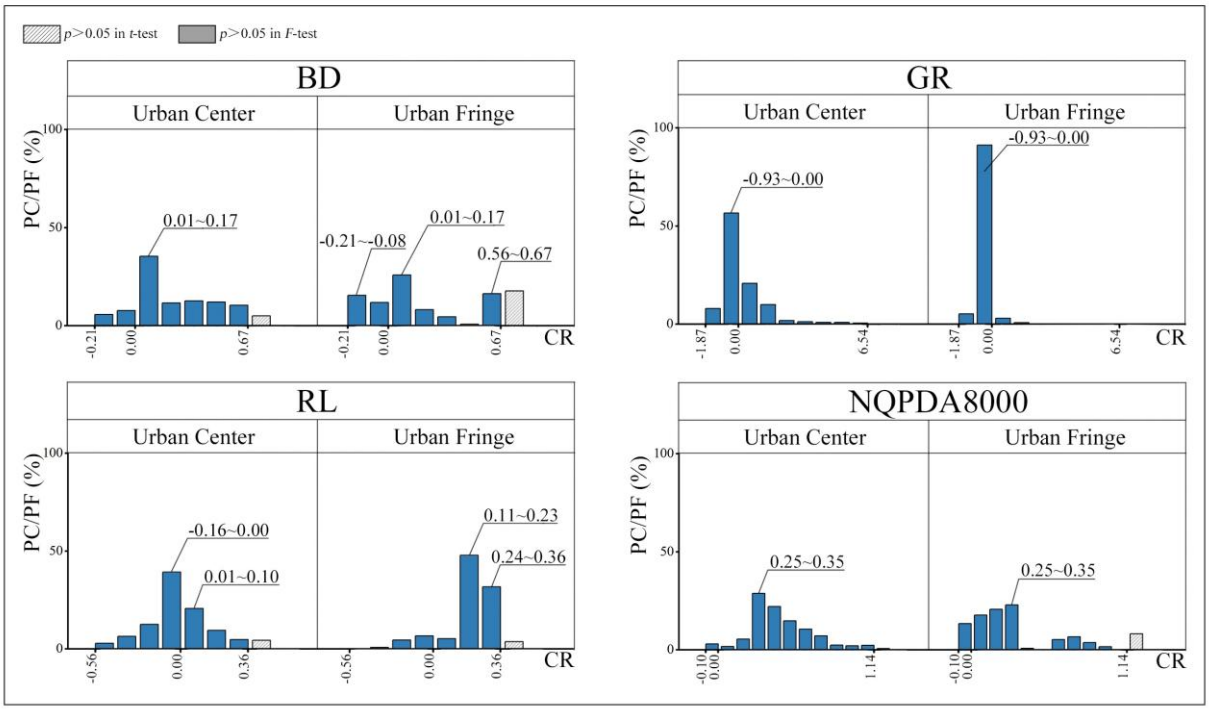

(a) 300 m

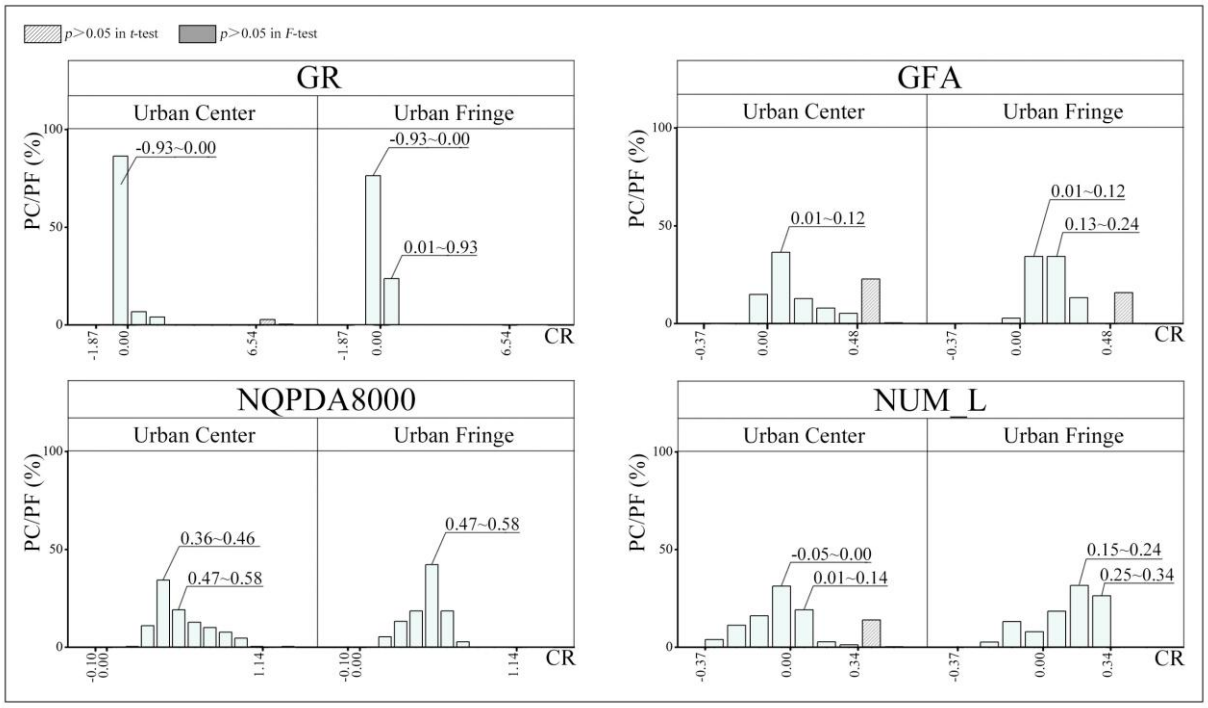

(b) 600 m

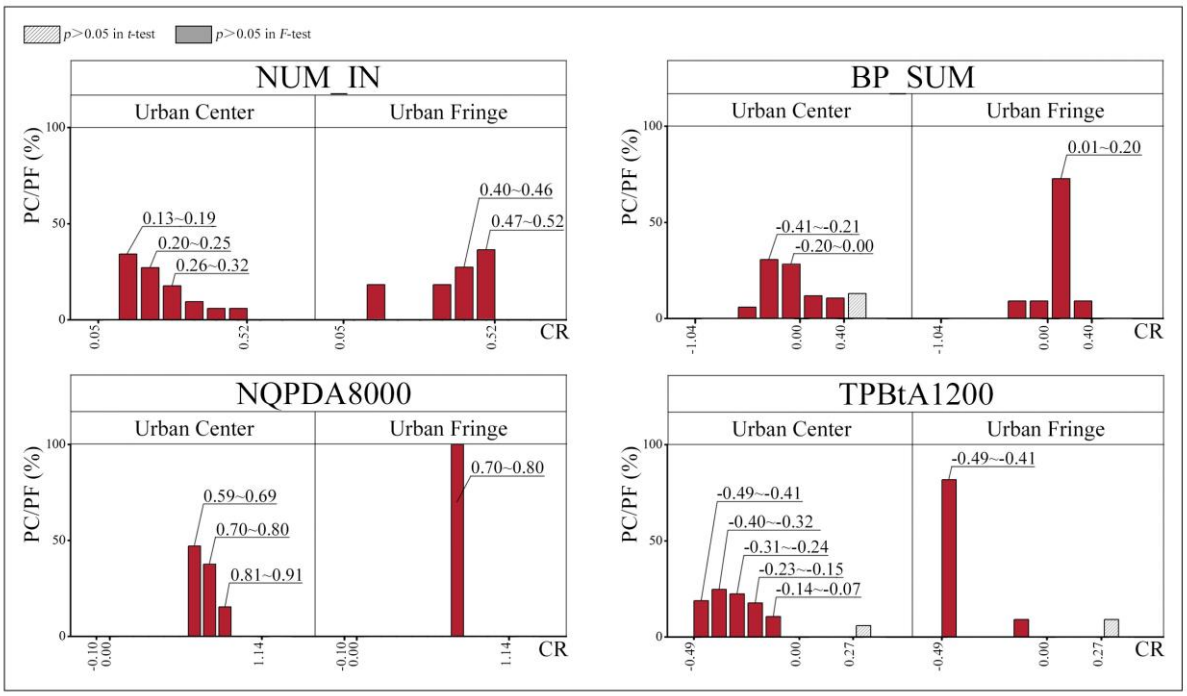

(c) 1200 m

Fig. 8. Proportion of the impact of each planning variable on traffic noise level in urban centre and fringe areas.

As displayed in Fig. 8a, at a scale of 300 m, the impact of BD on SPL in the urban centre mainly ranged from 0.01 to 0.17, accounting for 35.28% of the urban centre area. In 81.8% of the urban centre area, BD and SPL were positively correlated, indicating that in most of the urban centres, an increase in building density led to an increase in traffic noise level, which contradicted the previous research conclusion that 'building density and traffic noise are negatively correlated' (Montalvao Guedes et al., 2011; Ryu et al., 2017; Salomons and Pont, 2012; Weber et al., 2014). This could be attributed to the complex influencing factors of SPL in the urban centre: as illustrated in Fig. 5a, at the scale of 300 m, BD was significantly positively correlated with NQPDA8000 and significantly negatively correlated with GR, with Pearson coefficients of 0.22 and –0.35 respectively, indicating that places with high building density tended to have high car accessibility and low greening rate, which weakened the impact of BD on SPL. In the urban fringe, the impact of BD on SPL had the largest proportion in three coefficient ranges, which were 0.01–0.17, 0.56–0.67, and –0.21 to –0.08, respectively. Overall, the impact of BD in the urban centre was greater than that in the urban fringe, and previous studies have demonstrated that in places with high building density, the correlation between building density and noise is stronger (Weber et al., 2014), which is similar to the results of previous studies. The impact of GR on SPL was concentrated in the range of –0.93 to 0.00, accounting for 56.51% of the urban centre area, which was similar to the previous research conclusion that increasing the greening rate can effectively reduce traffic noise levels (Margaritis et al., 2016). In the urban fringe area, the impact of GR on SPL was negatively correlated in 91.19% of the areas, with a coefficient range from –0.93 to 0.00, which was much higher than 56.51% in the urban centre area. This may be due to the complex functional division in urban centres, higher population density, and frequent daily-life activities that weakened the inhibitory effect of the green ratio on the traffic noise level. Supporting this notion, research by Margaritis and Kang (2017) indicates that an increase in urban green spaces can effectively control traffic noise levels in urban fringe areas. Previous studies reported that the length of primary roads in urban areas is positively correlated with traffic noise (Margaritis and Kang, 2016). In this study, RL was negatively correlated with SPL in 60.85% of the urban centre area and positively correlated with SPL in 84.60% of the urban fringe area. This may be attributed to traffic control in the urban centre area, where the road network was dense. In general, a longer road creates more complex routing behaviour, which increases the probability of random behaviour and traffic control, thereby reducing traffic noise. The urban fringe contained

mostly unobstructed primary and secondary roads, and the road network was relatively simple than that in urban centres, with low vehicle density and less random behaviour, resulting in longer roads with higher traffic volume and traffic noise. NQPDA8000 was positively correlated with SPL in 96.31% of urban centres and 66.78% of urban fringes, which was lower than the proportion in urban centres, indicating that car accessibility had a greater impact on traffic noise in urban centres. This may be due to the difference in road network complexity between urban centres and urban fringes, where the activities in the urban fringe were mainly transportation-oriented, and many areas had strong car accessibility, which exhibited similarity and generality across multiple locations in the urban fringe, thereby rendering the impact of car accessibility on traffic noise in urban fringes weaker than in urban centres.

As portrayed in Fig. 8b, at a scale of 600 m, GR posed a predominant impact on SPL in urban centres, ranging from −0.93 to 0.00 and accounting for 86.37% of the urban centre area. Conversely, in the urban fringe, a negative correlation was observed between GR and SPL in 76.28% of the areas. Within urban centres, the GFA and SPL were positively correlated, accounting for 62.12% of the urban centre area, whereas in the urban fringe, such a positive correlation was present in 69.7% of the areas. Contrary to previous studies that failed to identify a significant correlation between traffic noise and gross floor area (Hong and Jeon, 2017), this study yielded different conclusions for two reasons. First, the previous study employed a smaller scale of 150 m × 150 m, whereas this study utilised a larger scale of 600 m × 600 m, as indicated by the GWR results, thereby strengthening the impact of GFA on SPL with scale expansion. Consequently, a positive correlation between the GFA and SPL was observed herein. Second, Fig. 8b depicted areas where the impact of GFA was not statistically significant ($p > 0.05$ in *t*-test), situated at the boundary between positive and negative impacts of GFA. Thus, the previous study presumably focused on these specific areas, resulting in insignificant effects. In all areas, NQPDA8000 exerted a positive impact on SPL. The regression coefficient for NUM_L in urban centres primarily fluctuated in the neighbourhood of 0, indicating a minimal impact on SPL. Conversely, in the urban fringe, the impact of NUM_L on SPL ranged from 0.15 to 0.34, encompassing 57.87% of the urban fringe area. Evidently, the influence of NUM_L on traffic noise levels was more pronounced in the urban fringe than urban centres, attributable to the lesser activity and fewer complex factors affecting traffic noise in the fringe areas.

As illustrated in Fig. 8c, NUM_IN exhibited a positive correlation with SPL in all areas at a scale of 1200 m, indicating that an increase in NUM_IN in either the urban centres or urban fringes increased the SPL. This finding aligns with previous research, which concluded that local road intersections contribute to elevated traffic noise levels (Margaritis and Kang, 2016). Additionally, the coefficient of NUM_IN predominantly ranged between 0.13–0.32 in urban centres and 0.40–0.52 in urban fringes. This suggests that the impact of NUM_IN on SPL is significantly greater in the urban fringes than in urban centres. The complex influencing factors present in urban centres potentially mitigate the effect of NUM_IN. Therefore, the impact of NUM_IN on SPL is much greater in the urban fringe than in the urban centre. Within the urban centres, approximately 64.71% of the areas exhibited a negative impact of BP_SUM on SPL, whereas in the urban fringes, 81.77% of the areas displayed a positive correlation between BP_SUM and SPL. This indicates that the impact of BP_SUM on SPL was predominantly negative in urban centres and predominantly positive in urban fringes. These findings contradict previous research conducted by Margaritis and Kang (2016), who reported that a larger building total perimeter corresponded to higher levels of traffic noise in the urban centre and fringe areas of Sheffield, UK. The disparity in findings may be attributed to variations in urban design across different countries. NQPDA8000 exhibited a positive impact on SPL in all areas, with a more concentrated effect observed on the urban fringe. This may be attributed to the relatively simplified influencing factors present in the urban fringe. Conversely, TPBtA1200 displayed a negative correlation with SPL in all areas, with the degree of impact ranging from −0.49 to −0.07 in urban centres and concentrated within the −0.49 to −0.41 range in the urban fringe. The negative correlation of TPBtA1200 is driven by different factors in urban centres and fringe areas. In urban centres, factors such as traffic control contribute to the imposition of restrictions on traffic noise in

areas with a high pedestrian passing probability, resulting in varying regression coefficients. Thus, the higher the pedestrian passing probability in the urban centre, the lower the traffic noise, leading to more diverse degrees of impact. Conversely, the urban fringe was predominantly characterised by highways and vehicular traffic. Areas with a high pedestrian passing probability tend to be situated further away from highways. Consequently, in the urban fringe, a higher pedestrian passing probability corresponds to lower traffic noise levels, resulting in a more concentrated impact degree.

4.3. The difference of planning variables' impact on traffic noise level at different scales

To investigate the impact of each planning variable on traffic noise at different scales, the coefficient values of each independent variable in the GWR model at different scales were statistically analysed. Fig. 9 depicts the variation in the impact of each planning variable on traffic noise in the regression model at different scales.

Fig. 9. Variations in the impact of planning variables on traffic noise level with scale

In Fig. 9, the average impact of BP_SUM on SPL increased gradually with an increase in scale. The average impact of the GFA was greater at the scale of 600 m than at the scale of 300 m, and the average impact was positive at the scale of 600 m, with a coefficient of 0.09, whereas the average impact was negative at the scale of 300 m, with a coefficient of –0.08. The impact of BS on the SPL exhibited a marginal decrease followed by an increase with an increase in scale. The average coefficient of RL decreased gradually with an increase in scale; all were negatively correlated, and the degree of negative correlation increased gradually. Although NUM_IN initially increased, it later decreased. The regression coefficients of GR decreased with an increase in scale, being 0.14, –0.04, and –0.26, respectively, at scales of 300, 600, and 1200 m, and the impact

degree initially weakened before increasing. This finding differed from that stated in previous research, where Margaritis and Kang (2017) reported that the correlation between green space indicators and noise decreased gradually from micro- to macroscopic levels. This disparity may arise from the fact that previous studies explored the variation of single variables with scale, while in this paper's regression model, GR is affected by other independent variables at different scales, thus altering the variation pattern. The average coefficient of TPBtA1200 decreased with the scale and was negatively correlated with the SPL. Moreover, NQPDA8000 positively impacted the SPL and increased with scale. The coefficients of NQPDA1200 and TPBtA8000 did not vary significantly at the different scales. The coefficients of the POI variables were generally approximate to zero and varied marginally at various scales.

4.4. Urban sound environment optimisation strategies and simulation verification from a planning perspective

This study proposed urban design strategies for general sound environment optimisations at different scales based on the average regression coefficient of each independent variable in the GWR model in Section 4.1.3. At the 300 m scale, the building total perimeter (BP_SUM) was increased, and car accessibility was reduced (NQPDA8000). At the 600 m scale, car accessibility (NQPDA8000) was reduced, the building total perimeter (BP_SUM) was increased, and the number of intersections (NUM_IN) was reduced. At the 1200 m scale, car accessibility (NQPDA8000) and the average building perimeter (BP_AVG) decreased, the road length (RL) of carriageways and the greening rate (GR) increased, and the number of intersections (NUM_IN) was reduced.

Additionally, based on the results of Section 4.2 and the local coefficients of the GWR model, we proposed refined design strategies for urban centres and fringes at different scales. For urban centres at the 300 m scale, it is recommended to reduce the building density (BD) and increase greening (GR) in the original building locations and other areas. Furthermore, increasing the road length (RL) of main roads and reducing car accessibility (NQPDA8000) is advised. At the 600 m scale, it is suggested to decrease gross floor area (GFA), enhance greening (GR) in vacant areas, reduce car accessibility (NQPDA8000), and increase the number of leisure POIs (NUM_L). Finally, the strategies proposed for the 1200 m scale involved reducing the number of road intersections (NUM_IN) and car accessibility (NQPDA8000), as well as increasing the pedestrian road probability (TPBtA1200) and building total perimeter (BP_SUM). For urban fringes at a 300 m scale, the building density (BD) was reduced, and urban greening (GR) was increased. In addition, car accessibility (NQPDA8000) was increased, and the carriageways (RL) were shortened. At the 600 m scale, the gross floor area (GFA) reduced, urban greening (GR) increased, car accessibility (NQPDA8000) diminished, and leisure POI number (NUM_L) decreased. At the 1200 m scale, the intersection number (NUM_IN) and car accessibility (NQPDA8000) increased the pedestrian road probability (TPBtA1200) and reduced the total building perimeter (BP_SUM).

To verify the feasibility and applicability of the aforementioned strategies, this study considered Shanghai, China as an example. The urban sound environment before and after optimisation is simulated using the noise simulation software Cadna/A, and fitting and comparison analyses are conducted using SPSS. The Hongkou District of Shanghai serves as the verification object for general design strategies at different scales. For the strategies in urban centres and fringes, the Huangpu District of Shanghai's urban centre and Songjiang District of its urban fringe were selected as the verification objects in accordance with *the provisions of Shanghai Urban Master Plan (2017–2035)*. Verification areas of 300 m × 300 m, 600 m × 600 m, and 1200 m × 1200 m were randomly selected within the verification objects, urban planning was redesigned according to the aforementioned strategies in these areas, and the optimisations effects were verified. The verification results are presented in Table 4.

Table 4. Simulation verification of urban sound environment optimisation strategies from the perspective of planning.

			Verification area	Before optimisation	After optimisation	Fitting curves before and after optimisation
Legend				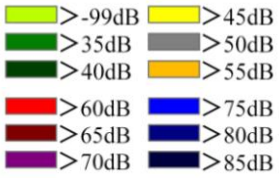		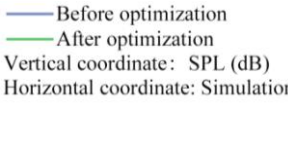
General sound environment optimisation strategies		300 m				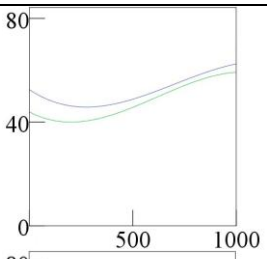
		600 m				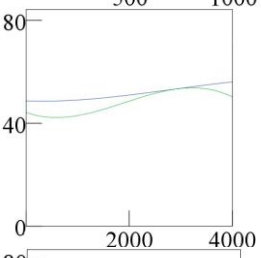
		1200 m				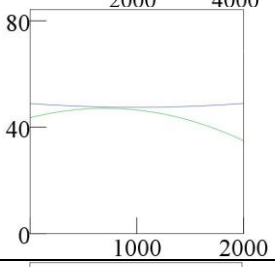
Sound environment optimisation strategies in urban centre and urban fringe	Urban centre	300 m				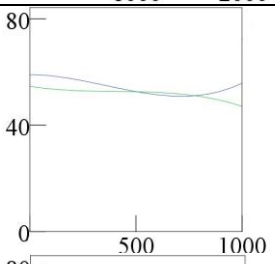
		600 m				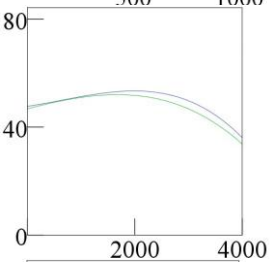
		1200 m				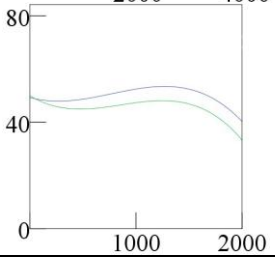

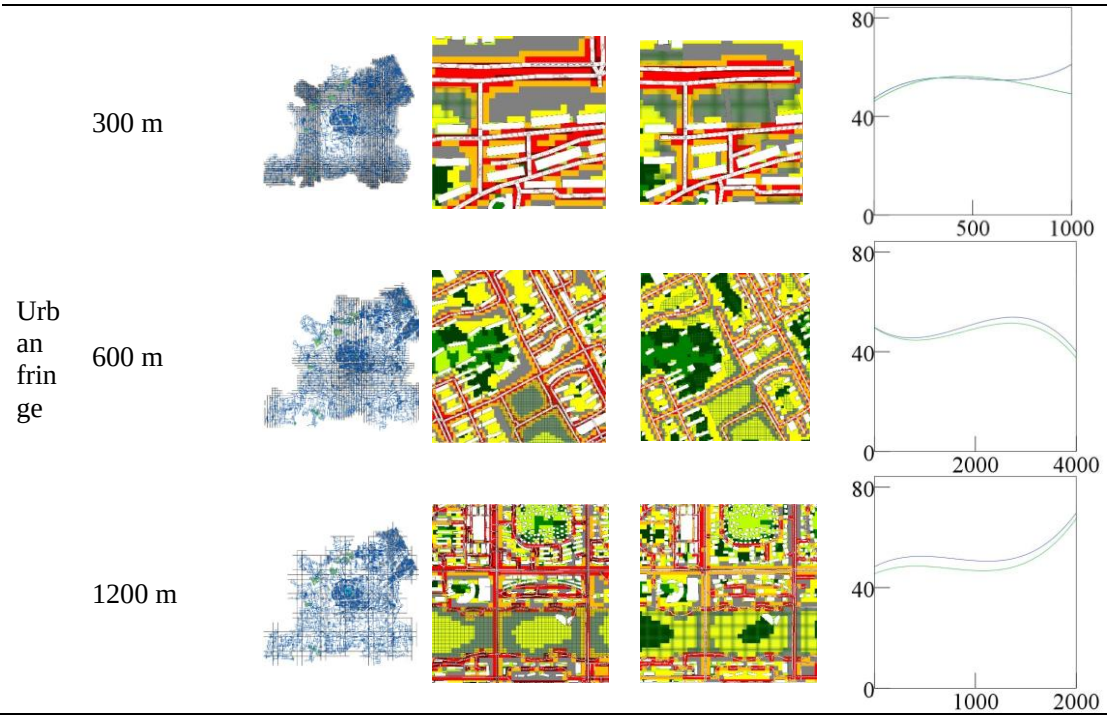

The fitting curves of the scatter plots before and after optimisation demonstrated that the proposed methods effectively reduced the traffic noise in the verification area. Furthermore, we evaluated percentage of noise reduction and noise reduction value based on the noise data before and after optimisation. The Cadna/A simulation employs a grid-based approach to approximate the noise level distribution across the entire area by calculating the average sound pressure level for each grid cell. The average values of the grid sound levels before and after optimization are calculated, and the difference is calculated to obtain noise reduction value, indicating the range of noise reduction. Percentage of noise reduction is the proportion of the grid cells with reduced noise after optimization, indicating the degree to which the optimization strategy can improve the regional noise. For general design strategies, at the 300 m scale, there was a 79.0% reduction in traffic noise with an average reduction of 4.2 dB. At the 600 m scale, a 57.7% reduction in traffic noise was observed, with an average reduction of 3.2 dB. At the 1200 m scale, a 62.1% reduction in the traffic noise was achieved, with an average reduction of 2.3 dB. Regarding design strategies by area, in urban centres at the 300 m scale, there was a 77.1% reduction in traffic noise with an average reduction of 1.9 dB. At the 600 m scale, an 87.9% reduction in traffic noise was recorded, with an average reduction of 1.6 dB. At the 1200 m scale, a 65.1% reduction in the traffic noise was observed, with an average reduction of 4.0 dB. In urban fringes at the 300 m scale, a 51.4% reduction in traffic noise was achieved, with an average reduction of 0.9 dB. At the 600 m scale, an 81.5% reduction in traffic noise was attained, with an average reduction of 1.7 dB. At the 1200 m scale, a 95.0% reduction in the traffic noise was observed, with an average reduction of 3.7 dB.

The noise reduction values for the general design strategies ranged from 2.3 to 4.3 dB, whereas the values for area-specific design strategies were between 1.6 and 4.0 dB for urban centres and between 0.9 and 3.7 dB for urban fringes. These results can be interpreted in the context of psychoacoustic phenomena. According to the classic psychoacoustic experiment known as "just noticeable difference (jnd)," the smallest perceivable change in sound level is dependent upon both the intensity and frequency of the sound (Long, 2014). Prior research indicates that the frequency of traffic noise predominantly falls within the 500 Hz to 2500 Hz range (Wang et al., 2019). Given that the traffic noise levels obtained from simulations in this study ranged approximately between 30 and 70 dB, the minimum sound level variation

perceptible to humans is estimated to be between 0.33 and 1.2 dB (Long, 2014). Consequently, the sound level reductions achieved through the implementation of these strategies are perceptible to human observers.

Moreover, extant research suggests that sustained noise reduction measures contribute to various health benefits, including a lowered incidence of hypertension and coronary heart disease (Swinburn et al., 2015). Additionally, such measures have been shown to enhance memory accuracy, thereby potentially improving work efficiency (Meng et al., 2021). Thus, the observed noise reductions not only have immediate perceptual implications but also offer long-term benefits in terms of both health and cognitive performance.

4.5. Limitations and prospects of the study

This study is subject to several limitations. Owing to the absence of high-spatial-resolution acoustic datasets, a software simulation method was employed to generate the acoustic data. Although Cadna/A is known for its high simulation accuracy, there may still exist slight errors in the actual sound pressure level. Moreover, the study area was limited in scope, and the research scale was restricted to only three scale sizes: 300, 600, and 1200 m. This limitation was primarily driven by considerations of workload and sample size. To gain a more comprehensive understanding of the influence of planning variables on traffic noise levels with relation to scale difference, future studies should encompass larger research areas and incorporate additional spatial scales. Furthermore, this study focuses on urban morphological variables, neglecting the potential impact of geodemographic factors on traffic noise. Previous studies have highlighted the relevance of variables such as population density and car availability ratio in determining noise levels (Margaritis and Kang, 2016; Ryu et al., 2017; Salomons and Pont, 2012). Hence, subsequent research could benefit from exploring the effects of these geodemographic factors on traffic noise across various urban areas and scales, thereby facilitating the development of more precise noise prediction models. Finally, this study verified the feasibility of utilising urban big data analysis for traffic noise and establishes the foundation for a machine-learning-based noise-prediction model that utilises urban big data as input.

5. Conclusions

In the context of smart cities, this study assessed the impact of planning variables on traffic noise levels at different scales using spatial statistics and other methods. The applicability of traditional planning variables and big data was compared for analysing traffic noise at various scales. Furthermore, this study examined the variations in the impact of planning variables on traffic noise across urban and fringe areas and the quantified the variations in their impact at these scales. The major conclusions of this study are stated as follows:

(1) The correlation between planning big data and traffic noise levels was stronger than that between traditional planning variables and traffic noise levels. Planning big data significantly affected the spatial heterogeneity of traffic noise levels. However, among the multi-parameter contributions, except for Closeness at 8000 m (car accessibility), the impact of other planning big data on traffic noise was observed to be less than that of the traditional planning variables.

(2) In urban centres and fringes, the impact of most key planning variables on traffic noise exhibited significant differences at the statistical level. For example, at a 300 m scale, the greening rate was negatively correlated with traffic noise in 91.19% of the range in urban fringes and only 56.51% in urban centres. Building density had a greater impact on traffic noise levels in urban centres than in urban fringes at the 300 m scale. At the 1200 m scale, the building total perimeter was mainly negatively correlated with traffic noise in urban centres and was positively correlated in urban fringes. The number of intersections posed a greater impact on traffic noise in urban fringes than in urban centres at the 1200 m scale.

(3) The average impact of the planning variables on the traffic noise level varied at different scales. For example, the average regression coefficient of the greening rate shifted from positive to negative upon increasing the scale and became negatively correlated with the traffic noise level at the 600 m scale. Closeness at 8000 m was positively correlated with the traffic noise level at all three scales, and its influence increased with scale, indicating that car accessibility played a more

decisive role in traffic noise levels at larger scales.

(4) This study proposed sound environment optimisation strategies for urban areas at various scales. The simulations verified that these strategies could reduce traffic noise by more than 50% in the study area, with certain strategies achieving an optimisation effect of more than 90%, thereby indicating adequate optimisation.

This study provided strategic support for noise control in urban design and guidance for the sound environment prediction of future unbuilt urban spaces. In addition, this study verified the applicability of planning big data for traffic noise analysis and provided support for future research on the optimisation of the sound environment in smart cities. Future studies should include larger research areas and diverse spatial scales to more comprehensively understand the influence of planning variables on traffic noise levels with scale alterations. Further research could focus on establishing a machine-learning noise prediction model using urban big data as input.

Acknowledgements

This work was supported by the National Natural Science Foundation of China (NSFC) [grant number 52178070 and 52208101], the Open Fund Project of Anhui Provincial Key Laboratory of Building Acoustic Environment [grant number AAE2021ZD03], the Shanghai Key Laboratory of Urban Design and Urban Science, NYU Shanghai, and Open Topic Grants [grant number 2022QMeng_LOUD].

References

OpenData V5.0. Introduction of open data for GPS floating cars in Dongguan demonstration area. OpenITS Organization.

FACT SHEET: Administration Announces New “Smart Cities” Initiative to Help Communities Tackle Local Challenges and Improve City Services. 2015, 2015.

Aiello LM, Schifanella R, Quercia D, Aletta F. Chatty maps: constructing sound maps of urban areas from social media data. Royal Society Open Science 2016; 3.

Aletta F, Margaritis E, Filipan K, Romero VP, Axelsson Ö, Kang J. Characterization of the soundscape in Valley Gardens, Brighton, by a soundwalk prior to an urban design intervention. Proceedings of the Euronoise Conference, 2015, pp. 1547-1552.

Alhazzani M, Alhasoun F, Alawwad Z, Gonzalez MC. Urban attractors: Discovering patterns in regions of attraction in cities. Plos One 2021; 16.

Bafna S. Space syntax: A brief introduction to its logic and analytical techniques. Environment and Behavior 2003; 35: 17-29.

Barrigon Morillas JM, Rey Gozalo G, Montes Gonzalez D, Atanasio Moraga P, Vilchez-Gomez R. Noise Pollution and Urban Planning. Current Pollution Reports 2018; 4: 208-219.

Borsekova K, Korony S, Vanova A, Vitalisova K. Functionality between the size and indicators of smart cities: A research challenge with policy implications. Cities 2018; 78: 17-26.

Cooper CHV, Chiaradia AJF. sDNA: 3-d spatial network analysis for GIS, CAD, Command Line & Python. Softwarex 2020; 12.

Ding L, Huang Z, Xiao C. Are human activities consistent with planning? A big data evaluation of master plan implementation in Changchun. Land Use Policy 2023; 126.

Dzhambov AM, Dimitrova DD, Turnovska TH. Improving traffic noise simulations using space syntax: preliminary results from two roadway systems. Arhiv Za Higijenu Rada I Toksikologiju-Archives of Industrial Hygiene and Toxicology 2014; 65: 259-272.

Hao Y, Kang J, Krijnders D, Wortche H. On the Relationship between Traffic Noise Resistance and Urban Morphology in Low-Density Residential Areas. Acta Acustica United with Acustica 2015; 101: 510-519.

Hong JY, Jeon JY. Relationship between spatiotemporal variability of soundscape and urban morphology in a multifunctional urban area: A case study in Seoul, Korea. Building and Environment 2017; 126: 382-395.

Huang B, Wu B, Barry M. Geographically and temporally weighted regression for modeling spatio-temporal variation in house prices. International Journal of Geographical Information Science 2010; 24: 383-401.

Huang M, Chen L, Zhang Y. A spatio-temporal noise map completion method based on crowd-sensing. Environmental Pollution 2021; 274.

Jackson HB, Fahrig L. Are ecologists conducting research at the optimal scale? Global Ecology and Biogeography 2015; 24: 52-63.

Kothari CL, Paul R, Dormitorio B, Ospina F, James A, Lenz D, et al. The interplay of race, socioeconomic status and neighborhood residence upon birth outcomes in a high black infant mortality community. SSM - population health 2016; 2: 859-867.

Lam K-C, Ma W, Chan PK, Hui WC, Chung KL, Chung Y-tT, et al. Relationship between road traffic noisescape and urban form in Hong Kong. Environmental Monitoring and Assessment 2013; 185: 9683-9695.

Lei Y, Flacke J, Schwarz N. Does Urban planning affect urban growth pattern? A case study of Shenzhen, China. Land Use Policy 2021; 101.

Levinson DM. Fundamentals of Transportation. LibreTexts, 2022.

Long M. 3 - Human Perception and Reaction to Sound. In: Long M, editor. Architectural Acoustics (Second Edition). Academic Press, Boston, 2014, pp. 81-127.

Luo Y, He J. Evaluating the heat island effect in a planned residential area using planning indicators. Journal of Building Engineering 2021; 43.

Ma F. Spatial equity analysis of urban green space based on spatial design network analysis (sDNA): A case study of central Jinan, China. Sustainable Cities and Society 2020; 60.

Margaritis E. Relationship Between Green Space-Related Variables and Traffic Noise Distribution in the Urban Scale, an Overall Approach. Inter Noise & Noise Con Congress & Conference Proceedings 2016.

Margaritis E, Filipan K, Kang J, Botteldooren D. The influence of vegetation and shape-related features in making parks more noise resistant. INTER-NOISE and NOISE-CON Congress and Conference Proceedings, 2016.

Margaritis E, Kang J. Effects of open green spaces and urban form on traffic noise distribution. Forum Acusticum 2014, 2014.

Margaritis E, Kang J. Relationship between urban green spaces and other features of urban morphology with traffic noise distribution. Urban Forestry & Urban Greening 2016; 15: 174-185.

Margaritis E, Kang J. Relationship between green space-related morphology and noise pollution. Ecological Indicators 2017; 72: 921-933.

Margaritis E, Kang J, Aletta F, Axelsson Ö. On the relationship between land use and sound sources in the urban environment. Journal of Urban Design 2020; 25: 629-645.

Margaritis E, Kang J, Filipan K, Botteldooren D. The influence of vegetation and surrounding traffic noise parameters on the sound environment of urban parks. Applied Geography 2018; 94: 199-212.

Meng Q, An Y, Yang D. Effects of acoustic environment on design work performance based on multitask visual cognitive performance in office space. Building and Environment 2021; 205.

Meng Q, Hu X, Kang J, Wu Y. On the effectiveness of facial expression recognition for evaluation of urban sound perception. Science of the Total Environment 2020; 710.

Mohareb N, Maassarani S. Assessment of street-level noise in three different urban settings in Tripoli. Urban Climate 2019; 29.

Montalvao Guedes IC, Bertoli SR, Zannin PHT. Influence of urban shapes on environmental noise: A case study in Aracaju - Brazil. Science of the Total Environment 2011; 412: 66-76.

Peng X, Bao Y, Huang Z. Perceiving Beijing's "City Image" Across Different Groups Based on Geotagged Social Media Data. Ieee Access 2020; 8: 93868-93881.

Popescu DI, Tuns RE, Moholea IF. The Urban Acoustic Environment - A Survey for Road Traffic Noise. Carpathian Journal of Earth and Environmental Sciences 2011; 6: 285-292.

Rey Gozalo G, Barrigon Morillas JM, Trujillo Carmona J, Montes Gonzalez D, Atanasio Moraga P, Gomez Escobar V, et al. Study on the relation between urban planning and noise level. Applied Acoustics 2016; 111: 143-147.

Ryu H, Park IK, Chun BS, Chang SI. Spatial statistical analysis of the effects of urban form indicators on road-traffic noise exposure of a city in South Korea. Applied Acoustics 2017; 115: 93-100.

Salomons EM, Pont MB. Urban traffic noise and the relation to urban density, form, and traffic elasticity. Landscape and Urban Planning 2012; 108: 2-16.

Schiff M, Hornikx M, Forssen J. Excess attenuation for sound propagation over an urban canyon. Applied Acoustics 2010; 71: 510-517.

Silva LT, Fonseca F, Rodrigues D, Campos A. Assessing the influence of urban geometry on noise propagation by using the sky view factor. Journal of Environmental Planning and Management 2018; 61: 535-552.

Song Y, Wang J, Ge Y, Xu C. An optimal parameters-based geographical detector model enhances geographic characteristics of explanatory variables for spatial heterogeneity analysis: cases with different types of spatial data. Giscience & Remote Sensing 2020; 57: 593-610.

Su K, Liao M, Li L, He Y, Deng S, Deng X. Traffic Noise Impact Prediction Based on Road Service Level. Transportation Research Record 2022; 2676: 480-488.

Suarez E, Barros JL. Traffic noise mapping of the city of Santiago de Chile. Science of the Total Environment 2014; 466: 539-546.

Swinburn TK, Hammer MS, Neitzel RL. Valuing Quiet An Economic Assessment of US Environmental Noise as a Cardiovascular Health Hazard. American Journal of Preventive Medicine 2015; 49: 345-353.

Tang L, Lin Y, Li S, Li S, Li J, Ren F, et al. Exploring the Influence of Urban Form on Urban Vibrancy in Shenzhen Based on Mobile Phone Data. Sustainability 2018; 10.

Tang UW, Wang ZS. Influences of urban forms on traffic-induced noise and air pollution: Results from a modelling system. Environmental Modelling & Software 2007; 22: 1750-1764.

Torija AJ, Ruiz DP, Ramos-Ridao A. Required stabilization time, short-term variability and impulsiveness of the sound pressure level to characterize the temporal composition of urban soundscapes. Applied Acoustics 2011; 72: 89-99.

Wang B, Kang J. Effects of urban morphology on the traffic noise distribution through noise mapping: A comparative study between UK and China. Applied Acoustics 2011; 72: 556-568.

Wang C, Yin L. Defining Urban Big Data in Urban Planning: Literature Review. Journal of Urban Planning and Development 2023; 149.

Wang H, Cai M, Cui H. Simulation and Analysis of Road Traffic Noise among Urban Buildings Using Spatial Subdivision-Based Beam Tracing Method. International Journal of Environmental Research and Public Health 2019; 16.

Wang H, Chen H, Cai M. Evaluation of an urban traffic Noise-Exposed population based on points of interest and noise maps: The case of Guangzhou. Environmental Pollution 2018; 239: 741-750.

Wang J-F, Zhang T-L, Fu B-J. A measure of spatial stratified heterogeneity. Ecological Indicators 2016; 67: 250-256.

Wang Q, Lu M, Li Q. Interactive, Multiscale Urban-Traffic Pattern Exploration Leveraging Massive GPS Trajectories. Sensors 2020; 20.

Weber N, Haase D, Franck U. Traffic-induced noise levels in residential urban structures using landscape metrics as indicators. Ecological Indicators 2014; 45: 611-621.

Wu H, Wang L, Zhang Z, Gao J. Analysis and optimization of 15-minute community life circle based on supply and demand matching: A case study of Shanghai. Plos One 2021; 16.

Yiannakou A, Salata K-D. Adaptation to Climate Change through Spatial Planning in Compact Urban Areas: A Case Study in the City of Thessaloniki. Sustainability 2017; 9.

Yin C, Yuan M, Lu Y, Huang Y, Liu Y. Effects of urban form on the urban heat island effect based on spatial regression model. Science of the Total Environment 2018; 634: 696-704.

Yu WL, Kang J. Relationship between traffic noise resistance and village form in China. Landscape and Urban Planning 2017; 163: 44-55.

Zhang Y, Zhao H, Li Y, Long Y, Liang W. Predicting highly dynamic traffic noise using rotating mobile monitoring and machine learning method. Environmental research 2023; 229: 115896-115896.

Zhong C, Arisona SM, Huang X, Batty M, Schmitt G. Detecting the dynamics of urban structure through spatial network analysis. International Journal of Geographical Information Science 2014; 28: 2178-2199.

Zhou Z, Kang J, Zou Z, Wang H. Analysis of traffic noise distribution and influence factors in Chinese urban residential blocks. Environment and Planning B-Urban Analytics and City Science 2017; 44: 570-587.